Investigation of a grid-free density functional theory (DFT) approach

Kurt R. Glaesemann and Mark S. Gordon

Citation: The Journal of Chemical Physics **108**, 9959 (1998); doi: 10.1063/1.476494
View online: http://dx.doi.org/10.1063/1.476494
View Table of Contents: http://scitation.aip.org/content/aip/journal/jcp/108/24?ver=pdfcov
Published by the AIP Publishing

Investigation of a grid-free density functional theory (DFT) approach

Kurt R. Glaesemann and Mark S. Gordon
Department of Chemistry and Ames Laboratory, United States Department of Energy, Iowa State University, Ames, Iowa 50011

(Received 28 January 1998; accepted 18 March 1998)

Density functional theory (DFT) has gained popularity, because it can frequently give accurate energies and geometries. Because evaluating DFT integrals fully analytically is usually impossible, most implementations use numerical quadrature over grid points, which can lead to numerical instabilities. To avoid these instabilities, the Almlöf-Zheng (AZ) grid-free approach was developed. This approach involves application of the resolution of the identity (RI) to evaluate the integrals. The focus of the current work is on the implementation of the AZ approach into the electronic structure code GAMESS, and on the convergence of the resolution of the identity with respect to basis set in the grid-free approach. Both single point energies and gradients are calculated for a variety of functionals and molecules. Conventional atomic basis sets are found to be inadequate for fitting the RI, particularly for gradient corrected functionals. Further work on developing auxiliary basis set approaches is warranted. © *1998 American Institute of Physics.* [S0021-9606(98)30124-5]

I. INTRODUCTION

In recent years, density functional theory (DFT), formulated in terms of the spin densities (n_α, n_β) representing all electrons, has gained popularity as a method for determining molecular properties and structures as an alternative to *ab initio* wave functions. Functionals of the density have been fit to the uniform electron gas,[1,2] and have incorporated corrections that depend upon the density gradient.[3–5] ''Hybrid functionals'' that mix in Hartree–Fock exchange can help correct for the inadequacies of a single-reference wave function, although the meaning of terms such as single-reference and multi-reference are not entirely clear for density functionals.[6,7] Nonetheless, a multi-reference wave function is still necessary for some problems, e.g., to describe bond breaking, and to obtain the correct electronic spin and space symmetry.[8,9] DFT can frequently give energies, relative energies, and geometries more accurately than second-order perturbation theory, with significantly less computational expense.[10] DFT can also give results in qualitative agreement with coupled cluster methods,[11] although reports of failures of DFT are not uncommon in the literature,[12–14] partially because DFT is not strictly variational.[15–17]

Integrating the functionals over the spin densities to obtain energies would require a computational effort of order N^4 or higher, where N is the size of the atomic basis set. Because evaluating integrals over the functionals in a closed analytic form is usually impossible, most DFT implementations evaluate the integrals using numerical quadrature over a finite set of grid points

$$\int_{\text{All space}} f(n_\alpha, n_\beta)\, d\mathbf{r} \approx \sum_{\text{Grid points}} f(n_\alpha, n_\beta)\, \Delta\mathbf{r}. \tag{1}$$

These grids are usually organized in atom centered Lebedev spheres.[18–20] Dunlap *et al.* eloquently discussed how the use of grids can lead to numerical instabilities.[21,22] Recently, grid-free approaches have been developed to avoid these difficulties.[21–25] However, these analytic approaches involve their own approximations, and their convergence with respect to basis set has not been explored extensively. The primary focus of the current work is on these basis set convergence properties of grid-free DFT. In Sec. II the Almlöf-Zheng (AZ) grid-free approach to DFT is discussed, with emphasis on its implementation into the electronic structure code GAMESS.[26] This will require calculating several types of integrals and doing several types of matrix manipulations. The derivation and implementation of analytic energy gradients are also discussed in this section. In Sec. III results based on the AZ approach are presented. Several prototypical systems are studied to explore the convergence of properties (geometries, dipole moments, singlet–triplet splittings, isomerization energies) as a function of the basis set. These results will demonstrate in detail the basis set dependence of the grid-free approach.

II. A GRID-FREE APPROACH TO DFT

A. Single point energies

In this section the AZ approach of using matrix relations to evaluate the complicated DFT integrals is explained. Initially methods of simplifying the integrals using approximations will be examined. This will result eventually in exactly evaluating a four-center integral and a gradient integral. The initial integral simplification uses the resolution of the identity RI.[27] Consider the product of two arbitrary functions, $f(x,y,z)$ and $g(x,y,z)$. In matrix representation the resolution of the identity can be expressed as

$$M_0[f \cdot g] \approx M_1[f] M_2[g], \tag{2}$$

where M_r are matrix representations in terms of some atomic basis set $\{\chi_i\}$. In terms of individual elements of the matrices (and therefore integrals)

$$M_0[f\cdot g]_{i,j}=\int \chi_i(f\cdot g)\chi_j d\mathbf{r}. \tag{3a}$$

$$\approx\sum_m \int \chi_i f\theta_m d\mathbf{r}\cdot\int \theta_m g\chi_j d\mathbf{r} \tag{3b}$$

$$=\sum_m M_1[f]_{i,m}M_2[g]_{m,j}. \tag{3c}$$

The foregoing expressions are exact if $\{\theta_m\}$ is a complete orthonormal set; otherwise, one expects some dependence of the calculations on the size of the basis set. Within GAMESS, the average of $f\bullet g$ and $g\bullet f$ is used, to preserve matrix symmetry. One well-defined choice for $\{\theta_m\}$ is the set of orthonormal molecular orbitals from the current self-consistent field (SCF) cycle. This choice appears to maintain a proportionality between the accuracy of the resolution of the identity and the accuracy of the wave function (the RI basis set and the atomic orbital basis set are the same size). As will be shown in Sec. III, this is unfortunately not the case.

As an example of using the resolution of the identity, consider the DePristo–Kress gradient corrected exchange functional,[28] which multiplies the uniform electron gas limit of $n^{4/3}$ times a term that depends on the gradient of the density. After substituting the density matrix D for one factor of n in Eq. (4a) and applying the resolution of the identity in Eq. (4b), this functional simplifies to

$$\int n^{\frac{3}{4}}y^2\,\frac{1+a_1y}{1+b_1y^2}\,d\mathbf{r}$$

$$=\sum_{\mu\nu}^{\text{AO's}} D_{\mu\nu}\cdot\int \chi_\mu n^{\frac{1}{3}}y^2\,\frac{1+a_1y}{1+b_1y^2}\,\chi_\nu d\mathbf{r} \tag{4a}$$

$$\approx\sum_{\mu\nu}^{\text{AO's}} D_{\mu\nu}\sum_m^{\text{Orthonormal}}\int \chi_\mu n^{\frac{1}{3}}\theta_m d\mathbf{r}$$

$$\cdot\int \theta_m y^2\,\frac{1+a_1y}{1+b_1y^2}\,\chi_\nu d\mathbf{r}, \tag{4b}$$

where a_1, b_1 = fitted parameters

$$y=\left|\frac{\nabla n}{n^{4/3}}\right|,$$

$$f(n)\ \text{ in Eq. (3)}=n^{\frac{1}{3}},$$

$$g(y)\ \text{ in Eq. (3)}=y^2\,\frac{1+a_1y}{1+b_1y^2}.$$

This leaves complicated integrals involving functions of the density n and the dimensionless density gradient y. Another resolution of the identity is used,[29] to evaluate these integrals, because they cannot be solved directly. This new resolution of the identity will rely upon the special properties of diagonalized matrices.

This resolution of the identity will transform $M[n]$ into $M[f(n)]$ for an arbitrary function f. Any function of the density, $f(n)$, may be represented in matrix form as follows. $M[n]$ is transformed into a new matrix $M'[n]$ using an orthonormal basis set

$$M'[n]=\tilde{V}M[n]V. \tag{5}$$

The matrix of LCAO coefficients is chosen for V, for which $\tilde{V}SV=I$, with S = overlap matrix in the atomic orbital basis set. $M'[n]$ is then diagonalized by a unitary transformation U, yielding eigenvalues λ

$$M'[n]=U\lambda\tilde{U}. \tag{6}$$

The function f is then evaluated at the eigenvalues, and incorporated into M'

$$M'[f(n)]\approx Uf(\lambda)\tilde{U}. \tag{7}$$

Equation (7) is exact in a complete basis (see Appendix A). Finally, $M'[n]$ is transformed back to the atomic basis, giving

$$M[f(n)]=(\tilde{V})^{-1}(Uf(\lambda)\tilde{U})(V)^{-1}=SVUf(\lambda)\tilde{U}\tilde{V}\tilde{S}. \tag{8}$$

Therefore, once the matrix representation of the density is determined, the matrix representation of any function of the density can be readily obtained. Similarly, this can be shown to be true for the matrix representations of y, n_α, or n_β.

The matrix representation of the density $M[n]$ is calculated from the first-order density matrix D and atomic orbitals i, j, k, and l, by

$$M[n]_{i,j}=\int \chi_i n\chi_j d\mathbf{r}$$

$$=\sum_{k,l} D_{kl}\int \chi_i\chi_k\chi_l\chi_j d\mathbf{r}=\sum_{k,l} D_{kl}(iklj). \tag{9}$$

The four-center one-electron integrals $(iklj)=\int\chi_i\chi_k\chi_l\chi_j d\mathbf{r}$ can be evaluated using a recursion formula similar to recursion formulas used by others[30,31]

$$\int \chi_a\chi_b\chi_c\chi_d d\mathbf{r}=(abcd)=\left(\frac{\alpha_aA_x+\alpha_bB_x+\alpha_cC_x+\alpha_dD_x}{\alpha_a+\alpha_b+\alpha_c+\alpha_d}-\alpha_aA_x\right)(a-1_x|\text{bcd})$$

$$+\frac{a_x(a-2_x|\text{bcd})+b_x(b-1_x|\text{acd})+c_x(c-1_x|\text{abd})+d_x(d-1_x|\text{abc})}{2(\alpha_a+\alpha_b+\alpha_c+\alpha_d)}, \tag{10}$$

where $\alpha_a,\alpha_b,\alpha_c,\alpha_d$ = Gaussian exponents

$A_x,B_x,C_x,D_x = X$ positions of atoms

with orbitals a, b, c, and d,

a_x,b_x,c_x,d_x = exponents of the x^0,x^1,x^2, etc.,

part of the orbital

(for $a=f_{x^2y}$ orbital: $a_x=2,a_y=1,a_z=0$).

Here, the integral $(b-1_x|\mathrm{acd})$ is the integral (abcd) with the x component of the angular momentum of orbital b decreased by one. Although the four-center one-electron integrals are unusual, they do appear in other contexts, such as the density based orbital localization method.[32,33] These one-electron integrals are analogous to the two-electron integral $\int\chi_i(1)\chi_k(1)(1/r_{12})\chi_l(2)\chi_j(2)d\mathbf{r}$ and are equivalent to the two-electron integral $\int\chi_i(1)\chi_k(1)\delta_{12}\chi_l(2)\chi_j(2)d\mathbf{r}$. The one-electron $(iklj)$ integrals formally scale computationally as order N^4, as do the corresponding two-electron integrals. Screening, parallelization, vectorization, direct, and symmetry techniques used to reduce the N^4 dependence of the two-electron $(i(1)k(1)|1/r_{12}|1(2)j(2))$ integrals[34] are easily extended to the $(iklj)$ integrals. For example, $(iklj)$ integrals can be screened to avoid their evaluation by using the Schwarz inequalities

$$(iklj)\leqslant\sqrt{(iikk)(lljj)}, \tag{11a}$$

$$(iklj)\leqslant\sqrt{(iill)(kkjj)}, \tag{11b}$$

$$(iklj)\leqslant\sqrt{(iijj)(kkll)}. \tag{11c}$$

Evaluation of the *set* of one-electron integrals takes less time than the set of two-electron integrals, because the index symmetries $[(iklj)=(ilkj)=\cdots]$ allow fewer unique integrals to be computed. Note, however, that the dominant time bottleneck is the number of indices, not whether the integral involves one or two electrons. The notion that one-electron integrals are significantly faster than two-electron integrals is historical, since usually one-electron integrals are of the type $(i\hat{h}j)$, where $\hat{h}$ = one-electron part of Hamiltonian operator. In the work of Almlöf and Zheng, these four-center one-electron integrals were approximated with three-center one-electron integrals, whose number grows as order N^3, using the resolution of the identity

$$(iklj)\approx\sum_m (ik\theta_m)(\theta_m lj). \tag{12}$$

This application of the resolution of the identity is computationally equivalent to expanding the density n in the $\{\theta_m\}$ basis and then calculating $M[n]$ (see Appendix B). This would result in a computational savings by reducing the number of integrals that have to be computed. In this work, $(ijkl)$ integrals are evaluated directly, although an option to use the three-center integral approximation has been implemented in GAMESS. Although the integrals scale as order N^4, the matrix multiplications and diagonalizations in the AZ grid-free approach scale as order N^3.

The more popular DFT functionals involve terms that depend upon the gradient of the density. Integrals over $|\nabla n|\cdot n^{-4/3}$ are computed as follows:

$$\int \chi_\mu\left(n^{-4/3}\frac{dn}{dx}\right)\chi_\nu d\mathbf{r}$$

$$=\int\chi_\mu\left(n^{-4/3}\frac{dn}{dx}-3n^{-1/3}\frac{d}{dx}\right)\chi_\nu\mathbf{r}$$

$$+\int\chi_\mu\left(3n^{-1/3}\frac{d}{dx}\right)\chi_\nu d\mathbf{r} \tag{13a}$$

$$=-3\int\chi_\mu\frac{d}{dx}(n^{-1/3}\cdot\chi_\nu)d\mathbf{r}+3\int\chi_\mu n^{-1/3}\frac{d}{dx}\chi_\nu d\mathbf{r} \tag{13b}$$

$$\approx 3\sum_m^{\text{Orthonormal}}\left(-\int\chi_\mu\frac{d}{dx}\theta_m d\mathbf{r}\cdot\int\theta_m n^{-1/3}\chi_\nu d\mathbf{r}\right.$$

$$\left.+\int\chi_\mu n^{-1/3}\theta_m d\mathbf{r}\cdot\int\theta_m\frac{d}{dx}\chi_\nu d\mathbf{r}\right) \tag{13c}$$

$$=-3\sum_m^{\text{Orthonormal}}\left(\int\chi_\mu\frac{d}{dx}\theta_m d\mathbf{r}\cdot\int\theta_m n^{-1/3}\chi_\nu d\mathbf{r}\right.$$

$$\left.+\int\chi_\nu\frac{d}{dx}\theta_m d\mathbf{r}\cdot\int\theta_m n^{-1/3}\chi_\mu d\mathbf{r}\right). \tag{13d}$$

The last step follows, because d/dx is anti-hermitian and $n^{-1/3}$ is hermitian. The $\int\chi_i d/dx\chi_j d\mathbf{r}$ are dipole velocity integrals. The d/dy and d/dz contributions are calculated similarly. We only study the gradient of the energy, because no popular functional uses higher order derivatives, due to numerical stability problems.[35,36]

In order to calculate energies, the wave function must be optimized using a (SCF) method. This requires calculating Fock matrix elements, which are the derivatives of the energy with respect to changing the orbitals. The contribution of functional $f(n_\alpha,n_\beta,\nabla n_\alpha,\nabla n_\beta)$ to the alpha Fock matrix is computed from the spin densities (n_α,n_β), and atomic orbitals χ_i,χ_j[37]

$$F_{ij}^{\mathrm{DFT},\alpha}=\int\left(\frac{\partial f}{\partial n_\alpha}(\chi_i\chi_j)+\frac{\partial f}{\partial\nabla n_\alpha}\nabla(\chi_i\chi_j)\right.$$

$$\left.+\frac{\partial^2 f}{\partial\nabla n_\alpha^2}\nabla^2(\chi_i\chi_j)+\cdots\right)d\mathbf{r}. \tag{14a}$$

A more easily coded, but less transparent formulation for the first two terms is[10]

$$F_{ij}^{\mathrm{DFT},\alpha}=\int\left(\frac{\partial f}{\partial n_\alpha}(\chi_i\chi_j)+2\frac{\partial f}{\partial(\nabla n_\alpha\cdot\nabla n_\alpha)}\nabla n_\alpha\right.$$

$$\left.+\frac{\partial f}{\partial(\nabla n_\alpha\cdot\nabla n_\beta)}\nabla n_\beta\right)\nabla(\chi_i\chi_j)d\mathbf{r}. \tag{14b}$$

It is important to note that (unlike traditional Hartree–Fock) the dot product of F^{DFT} with the density matrix does not give the DFT energy contribution; the DFT contribution to the energy must be explicitly calculated. For example, the dot

TABLE I. He energies in hartrees with the Slater exchange functional.

Basis set	Hartree–Fock	Grid	Grid free
5*s*	−2.858 589	−2.719 253	−2.722 985
10*s*	−2.861 647	−2.723 547	−2.723 952
15*s*	−2.861 679	−2.723 630	−2.723 731
20*s*	−2.861 680	−2.723 638	−2.723 674

TABLE II. Be energies in hartrees with the Slater exchange functional.

Basis set	Hartree–Fock	Grid	Grid free
5*s*	−14.479 361	−14.131 597	−14.156 690
10*s*	−14.571 727	−14.221 960	−14.224 846
15*s*	−14.572 985	−14.223 236	−14.223 890
20*s*	−14.573 021	−14.223 284	−14.223 487
25*s*	−14.573 023	−14.223 289	−14.223 369

product of the X-α Fock matrix with the density matrix would overestimate exchange by 1/3 (see Appendix C).

B. Analytic nuclear gradients of the energy

Chemists usually not only want the energy for a single arbitrary geometry, but the geometry at a stationary point on the potential energy surface as well. To efficiently search for these geometries, the derivative of the energy with respect to nuclear coordinates is needed. Although many DFT codes calculate these nuclear gradients, the potential energy surfaces sometimes suffer from grid noise.[21,22,24] Because the grid moves with the atoms, derivatives with respect to the grid are needed, but many DFT codes neglect these terms.[10,38,39] Such irregularities make determining saddle points and energy minima difficult. Methods for eliminating these effects have been developed.[40,41] However, the corrections can introduce numerical difficulties of their own, and therefore other research groups now advocate relying on tighter grids to eliminate these problems.[41,42]

The grid-free DFT approach can be extended to the computation of gradients as follows. The Hartree–Fock formalism for the derivative with respect to nuclear coordinate X_A for restricted closed shell noncomplex wave functions is

$$\frac{\partial E}{\partial X_A}=\left\langle \Psi\left(\frac{\partial H}{\partial X_A}\right)\Psi\right\rangle+4\sum_i^{\mathrm{occ}}\langle\psi_i'|(\hat{V}+\hat{T}+\hat{J}-\hat{K})-\epsilon_i|\psi_i\rangle, \tag{15}$$

where $\psi_i'=\Sigma_r^{\mathrm{AO}}C_{\mathrm{ri}}\partial\chi_r/\partial X_A$ and the other operators and symbols have their usual meaning: operators $\hat{V}$=nuclear-electron attraction, $\hat{T}$=kinetic energy, $\hat{J}$=Coulomb, $\hat{K}$=exchange; χ=atomic orbitals, Ψ=molecular wave function, ψ=spin orbitals, and ϵ_i=orbital energy. The sum of Eq. (15) is over occupied spin orbitals. Only the exchange term $\hat{K}$ in the resulting integral

$$\int\left(\frac{\partial\chi_r}{\partial X_A}\right)\hat{K}\chi_s d\mathbf{r} \tag{16}$$

must be modified to calculate DFT gradients. $\hat{K}$ is replaced with the DFT exchange-correlation term $\hat{K}^{\mathrm{DFT}}$. If atomic orbital χ_r is not on atom A, then the derivative is zero, because χ_r has no dependence on the position of atom A. If χ_r is centered on atom A, then the nuclear coordinate X_A is replaced by the negative of the electronic coordinate x. This is because X_A appears in the Gaussian basis function χ_r as $(x-X_A)$

$$\int\left(\frac{\partial\chi_r}{\partial X_A}\right)\hat{K}^{\mathrm{DFT}}\chi_s d\mathbf{r}=-\int\left(\frac{\partial\chi_r}{\partial x}\right)\hat{K}^{\mathrm{DFT}}\chi_s d\mathbf{r}. \tag{17}$$

The resolution of the identity is then applied, giving

$$\int\left(\frac{\partial\chi_r}{\partial X_A}\right)\hat{K}^{\mathrm{DFT}}\chi_s d\mathbf{r}\approx-\sum_m^{\mathrm{Orthonormal}}\int\left(\frac{\partial\chi_r}{\partial x}\right)\theta_m d\mathbf{r}\cdot\int\theta_m\hat{K}^{\mathrm{DFT}}\chi_s d\mathbf{r}. \tag{18}$$

Evaluation of both integrals in Eq. (18) is possible, because these are related to dipole velocity and the DFT contribution to the Fock matrix. It is important to realize that this approach is independent of the functional chosen. Once the grid-free gradients are implemented, they are available for all functionals for which single point energies are available. The resolution of the identity in Eq. (18) can introduce problems, if the basis set $\{\theta_m\}$ is inadequate. For example, the exchange-correlation contribution to a translation of the entire molecule in the x direction clearly must be zero

$$\delta T_x=4\sum_i^{\mathrm{occ}}\int\left(\sum_A^{\mathrm{atom}}\frac{\partial\psi_i}{\partial X_A}\right)\hat{K}^{\mathrm{DFT}}\psi_i d\mathbf{r}=-4\sum_i^{\mathrm{occ}}\int\left(\frac{\partial\psi_i}{\partial x}\right)\hat{K}^{\mathrm{DFT}}\psi_i d\mathbf{r}=0. \tag{19}$$

With the application of the resolution of the identity, this becomes

TABLE III. He energies in hartrees with the Becke88 exchange functional.

Basis set	Grid	Grid free (+1*p*)	Grid free (+3*p*)	Grid free (+5*p*)	Grid free (+10*p*)	Grid free (+15*p*)	Grid free (+20*p*)
5*s*	−2.859 231	−2.801 225	−2.845 034	−2.857 012			
10*s*	−2.863 302	−2.797 241	−2.848 139	−2.860 223	−2.863 275		
15*s*	−2.863 373	−2.796 592	−2.846 943	−2.860 447	−2.862 979	−2.863 351	
20*s*	−2.863 378	−2.796 338	−2.846 451	−2.858 871	−2.862 903	−2.863 271	−2.863 366

TABLE IV. Be energies in hartrees with the Becke88 exchange functional.

Basis set	Grid	Grid free $(+1p)$	Grid free $(+3p)$	Grid free $(+5p)$	Grid free $(+10p)$	Grid free $(+15p)$	Grid free $(+20p)$	Grid free $(+25p)$
10*s*	−14.564 943	−14.415 043	−14.500 901	−14.541 349	−14.565 649			
15*s*	−14.566 296	−14.417 206	−14.502 231	−14.540 217	−14.564 638	−14.566 347		
20*s*	−14.566 353	−14.415 954	−14.502 004	−14.538 576	−14.564 523	−14.565 936	−14.566 589	
25*s*	−14.566 362	−14.414 982	−14.501 644	−14.537 827	−14.564 432	−14.565 804	−14.566 240	−14.566 420

$$\delta T = -4\sum_{i}^{\text{occ}} \int \left(\frac{\partial \psi_i}{\partial x}\right)\hat{K}^{\text{DFT}}\psi_i d\mathbf{r} \approx -4\sum_{i}^{\text{occ}} \sum_{m}^{\text{Orthonormal}} \int \left(\frac{\partial \psi_i}{\partial x}\right)\theta_m d\mathbf{r} \cdot \int \theta_m \hat{K}^{\text{DFT}}\psi_i d\mathbf{r}, \tag{20}$$

which is not necessarily zero. This also applies to translations in the y and z directions, and to net rotations about the molecule's center of mass. These variances (which vanish in symmetric molecules), are projected out in GAMESS. This is done by summing all the contributions to a translation or torque and then subtracting it back out. This emphasizes the need for an adequate basis set $\{\theta_m\}$ to ensure that the resolution of the identity has been sufficiently converged. These variances are also present in the grid based approach, but are reported not to occur in the X-α specific approach of Werpetinski and Cook.[25] The sizes of the variances $\delta T_x, \delta T_y, \delta T_z, \delta R_x, \delta R_y, \delta R_z$ can be used as diagnostics for the adequacy of the basis set's capability to resolve the identity.

C. The grid connection

Now that the implementation of the grid-free approach is clearly laid out, it is worthwhile to examine its relationship to the grid based approach. Careful analysis reveals that the grid based approach may be thought of as a special case of the grid-free approach. Consider the generic integral $\int \chi_i f(n_\alpha)\cdot g(n_\beta)\chi_j d\mathbf{r}$. An auxiliary basis set of nonoverlapping normalized step functions $\{\theta_m\}$ is used for the resolution of the identity. The resolution of the identity as in Eq. (3), which is exact in a complete basis $\{\theta_m\}$, is applied, to give

$$\int \chi_i f(n_\alpha)\cdot g(n_\beta)\chi_j d\mathbf{r} \approx \sum_m \int \chi_i f(n_\alpha)\theta_m d\mathbf{r} \cdot \int \theta_m g(n_\beta)\chi_j d\mathbf{r}. \tag{21}$$

The atomic orbitals $\{\chi\}$ are assumed to vary insignificantly over an individual step function θ_m, therefore the atomic orbitals act like step functions in the region of θ_m. This gives

$$\int \chi_i f(n_\alpha)\cdot g(n_\beta)\chi_j d\mathbf{r} \approx \sum_m \xi_{i,m}\int \theta_m f(n_\alpha)\theta_m d\mathbf{r} \cdot \xi_{j,m}\int \theta_m g(n_\beta)\theta_m d\mathbf{r}, \tag{22}$$

where $\xi_{i,m}$ is a grid-size weighted overlap. For a fine grid, this is the value of the orbital χ_i at the step function θ_m multiplied by the size of θ_m. Now, the matrix function representation in Eq. (8), which is exact in a complete basis $\{\theta\}$, is used. Because $M[f(n_\alpha)]$ and $M[g(n_\beta)]$ are diagonal in the θ basis, $U=I$ in Eq. (8), so

$$\int \chi_i f(n_\alpha)\cdot g(n_\beta)\chi_j d\mathbf{r} \approx \sum_m \xi_{i,m}\xi_{j,m} f\left(\int \theta_m n_\alpha \theta_m d\mathbf{r}\right) \cdot g\left(\int \theta_m n_\beta \theta_m d\mathbf{r}\right). \tag{23}$$

If the grid of step functions is very tight, then the step function is a single grid point. This gives the integral in terms of a grid

TABLE V. Neon energies in hartrees with the Becke88 exchange functional.

Basis set	Grid	Grid free $(+0d)$	Grid free $(+1d)$	Grid free $(+3d)$	Grid free $(+5d)$	Grid free $(+10d)$
10*s*10*p*	−128.580 485	−128.337 180	−128.424 312	−128.538 924	−128.578 138	−128.584 228
15*s*10*p*	−128.589 469	−128.351 221	−128.436 205	−128.548 799	−128.582 479	−128.588 480
15*s*15*p*	−128.589 771	−128.352 051	−128.438 204	−128.549 564	−128.583 082	−128.589 235
20*s*10*p*	−128.589 749	−128.353 294	−128.438 981	−128.549 593	−128.582 621	−128.588 607
20*s*15*p*	−128.590 051	−128.354 483	−128.440 131	−128.550 023	−128.583 751	−128.589 404
20*s*20*p*	−128.590 069	−128.354 434	−128.440 120	−128.548 917	−128.583 121	−128.589 297
25*s*10*p*	−128.589 767	−128.354 170	−128.440 521	−128.549 615	−128.582 726	−128.588 583
25*s*15*p*	−128.590 069	−128.355 356	−128.441 362	−128.550 457	−128.583 821	−128.589 407
25*s*20*p*	−128.590 087	−128.355 502	−128.441 220	−128.548 636	−128.583 303	−128.589 306
25*s*25*p*	−128.590 090	−128.355 500	−128.441 166	−128.548 669	−128.583 157	−128.589 280

TABLE VI. CO and N_2 results with the Becke88 functional.

Atomic and molecular energies (hartree)	Grid	Grid free
C	−37.690 44	−37.688 25
O	−74.833 15	−74.829 51
CO	−112.873 14	−112.872 04
N	−54.400 88	−54.400 26
N_2	−109.086 20	−109.085 26
Binding energies (eV)		
N_2	7.68	7.75
CO	9.51	9.64
Bond lengths (Å)		
CO	1.147	1.148
N_2	1.113	1.113
Dipole moments (debye)		
CO	0.1655	0.1621

$$\int \chi_i f(n_\alpha)\cdot g(n_\beta)\chi_j d\mathbf{r} \approx \sum_m \xi_{i,m}\xi_{j,m} f(n_\alpha \text{ at grid point } m) \cdot g(n_\beta \text{ at grid point } m). \quad (24)$$

This is the grid based approach to evaluation of the integrals that arise in DFT.

III. GRID-FREE DFT RESULTS

A. Functionals and methods

The grid-free approach outlined in Secs. II and III is used to implement several DFT functionals in GAMESS:

(1) Local exchange: $X-\alpha$[1] which is exact in the limit of a uniform electron gas for $\alpha=2/3$. The more popular empirical value of $\alpha=0.7$ is also available if no gradient correction to exchange is present.
(2) Local correlation: VWN5[2,10] and the PW local,[43] which are designed to interpolate between the ferromagnetic limit and paramagnetic limit of the Ceperley and Alder[44] Monte Carlo results. The PW local approach is a newer more accurate fit that is reported to give overall better energetics and structures than the VWN fits.
(3) Local exchange and correlation: three Wigner forms,[43,45–47] which are designed to model exchange and correlation simultaneously. These are modifications of the simple, yet effective, equation

$$E_{xc}=\int \frac{C_1 n^{4/3}}{1+C_2 n^{1/3}}\, d\mathbf{r}, \quad (25)$$

which in the limit of $C_2=0$ is $X-\alpha$. The Wigner form does not involve any terms that depend upon the spin-polarization $\xi=(n_\alpha-n_\beta)/(n_\alpha+n_\beta)$; therefore, the portion of correlation that results from $\alpha-\beta$ interaction is not included.
(4) Gradient-corrected exchange: DePristo-Kress,[28] Becke88,[48] and the CAMA[43] and CAMB[43] modifications to Becke88. These all multiply a local exchange term by functions of the dimensionless density gradient $y=|\nabla n|/n^{4/3}$. Becke88 is by far the most popular functional.
(5) Closed shell gradient-corrected correlation: LYP[49,50] which is designed to reformulate the correlation formulas of Colle and Salvetti[51] in terms of the electron density and the local kinetic energy density. This functional is not based upon adding a correction term to a local correlation functional.

Naturally, combinations of these functionals, such as BVWN with Becke88 exchange and VWN correlation are available to the user. Hybrid functionals such as mixing half Hartree–Fock exchange and half Becke88 exchange are available also.

All comparisons presented below are made to the grid based DFT code in Gaussian 92/DFT.[52] A pruned (75,302) grid of approximately 7000 points per atom[53] is used, because looser grids gave off-axis dipole components for NH_3 and a net dipole moment for planar NH_3. Both GAMESS and Gaussian92/DFT calculate all nonexchange/correlation terms explicitly from Ψ, rather than from n and the dimensionless gradient y

TABLE VII. NH_3 and H_2O dipole moments with the Becke88 functional.

	H_2O grid free	H_2O grid dipole	NH_3 grid free	NH_3 grid
cc-VDZ	1.6675 D	1.8016 D	1.3818 D	1.5027 D
cc-VTZ	1.8415 D	1.8379 D	1.4935 D	1.5084 D
cc-VQZ	1.8057 D	1.8086 D	1.4912 D	1.4832 D
cc-VPZ	1.8140 D	1.8099 D	1.4690 D	1.4661 D

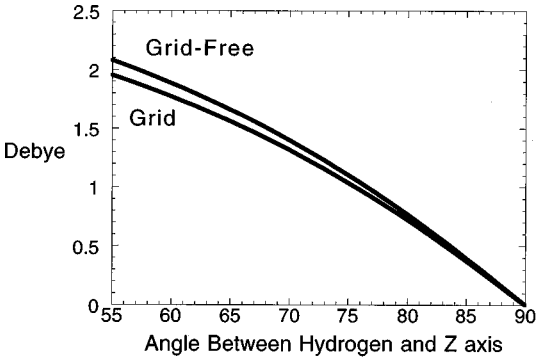

FIG. 1. NH_3 dipole with the Becke88 and $6-311++G(3d,3p)$.

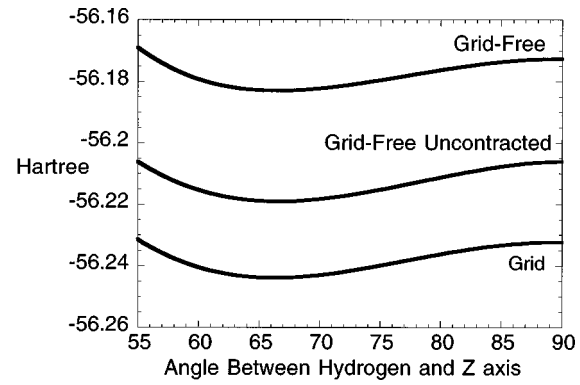

FIG. 2. NH_3 bend potential with the Becke88 and $6-311++G(3d,3p)$.

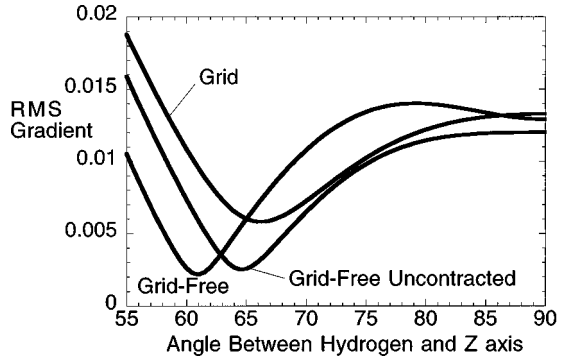

FIG. 3. NH_3 rms gradient with the Becke88 and $6-311++G(3d,3p)$.

$$E=\int [C_{\text{kinetic}}n^{5/3}+C_{\text{potential}}n+C_{\text{exchange}}n^{4/3}\cdot f(y)]d\mathbf{r},$$

$$\text{where } y=\left|\frac{\nabla n}{n^{4/3}}\right| \tag{26}$$

as was done in older purely DFT implementations. The current implementation of grid-free DFT in GAMESS does not use an auxiliary basis set, so the same basis that is used for the linear combination of atomic orbitals (LCAO) expansion is also used for the resolution of the identity. Consequently, as the basis set size is increased, both the accuracy of the wave function and the accuracy of the resolution of the identity are increased. Of course, use of an auxiliary basis set for the resolution of the identity would be more efficient and will be implemented in a subsequent version.

B. Energies of atoms

Small closed shell atoms provide a good initial test case. Absolute energies for atoms are calculated using even tempered uncontracted basis sets.[54,55] He, Be, and Ne are studied here. As can be seen in Tables I and II, the Slater functional (X-α with $\alpha=2/3$) energy converges with relatively small basis sets. Tables III–V show that gradient corrected functionals require basis functions of one higher angular momentum quantum number, because of the resolution of the identity introduced in Eq. (13d). When i and j are on the same atom, the integral $\int \chi_i d/dx \chi_j d\mathbf{r}$ vanishes if i and j do not differ by exactly one in x angular momentum. Even though s functions on Ne provide a gradient correction to the p functions, the addition of d functions greatly enhances the accuracy of the calculation, by providing an additional gradient correction as can be seen clearly in Table V. Although adding d functions to helium would make the basis set more complete (and therefore make the resolution of the identity more exact), it would not improve the accuracy of the calculation, unless the functional includes second derivatives of the density. This is because the second derivative of the density would involve $\int \chi_i d^2/dx^2 \chi_j d\mathbf{r}$ integrals and these vanish unless i and j have the same x angular momentum or differ by exactly two in x angular momentum.

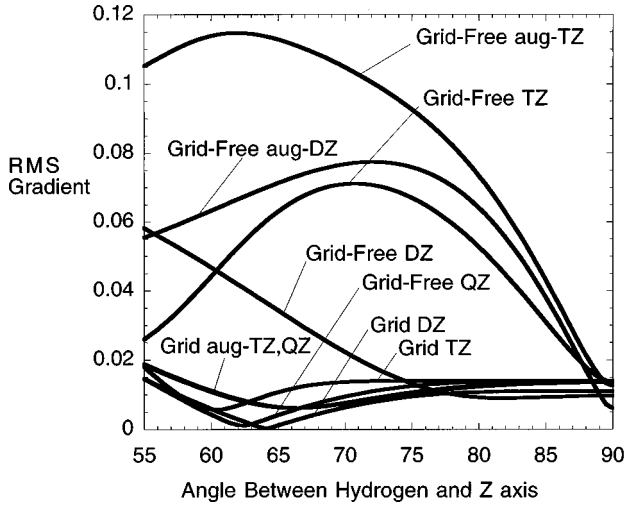

FIG. 5. NH_3 rms gradient with the Becke88 functional and correlation consistent basis sets.

C. Energies and dipole moments of diatomics

The bond distances, dipole moments, and binding energies for CO and N_2 calculated with the B-null (Becke88 exchange, no correlation) functional using uncontracted even tempered basis sets[54,55] are given in Table VI. The isolated atoms are calculated using unrestricted wave functions. The basis sets used are $20s13p10d3f$ for N, $20s13p10d1f$ for C, and $20s13p10d1f$ for O. The grid and grid-free results for both N_2 and CO are very comparable, differing by only 0.001 Å. Both approaches predict CO dipole moments that

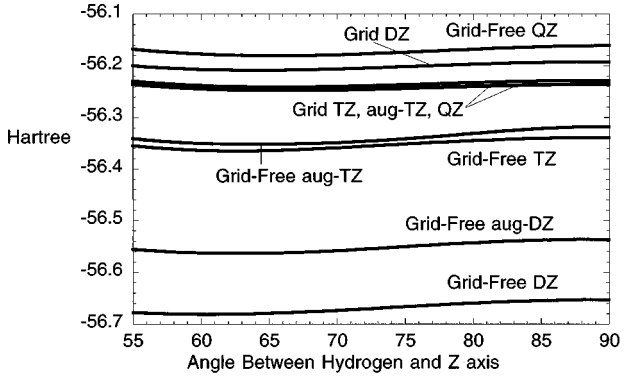

FIG. 4. NH_3 bend potential with the Becke88 functional.

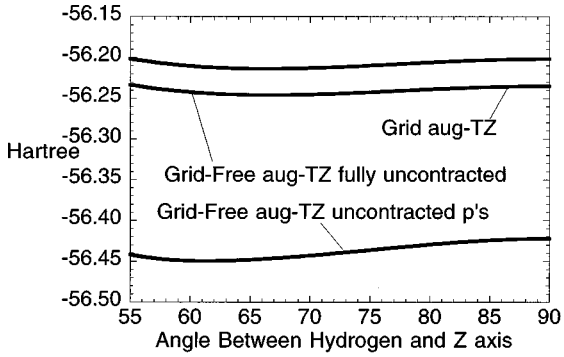

FIG. 6. NH_3 energy with the Becke88 functional and correlation consistent basis sets.

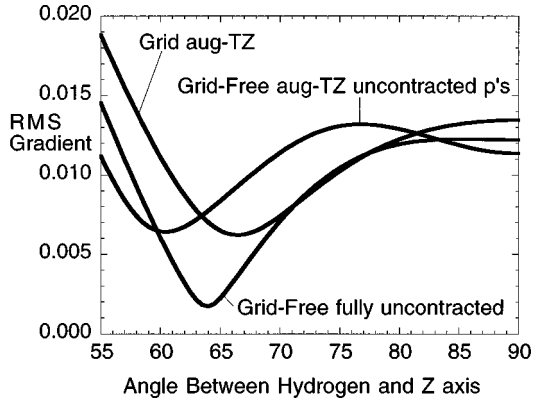

FIG. 7. NH_3 rms gradient with the Becke88 functional and correlation consistent basis sets.

are within 2% of each other. *B* null overestimates the N_2 bond length compared to the experimental[56] value of 1.098 Å, and underestimates the experimentally predicted[56] N_2 binding energy of 9.90 eV. This functional also overestimates the CO bond length compared to the experimental value of 1.128 Å,[57] and underestimates the experimentally predicted[58] CO binding energy of 11.1 eV. The sign of the CO dipole moment is predicted correctly (difficult to do[59,60]) and close to the experimental[61,62] value of 0.112 D.

D. Energies and dipole moments

Dipole moments and energies for H_2O and NH_3 are examined with *B*-null using correlation consistent[63] basis sets in Table VII. The water geometry is fixed at $R(\mathrm{OH}) = 0.957\,81$ Å, $\theta(\mathrm{HOH}) = 104.4776°$, and that of ammonia is fixed at $R(\mathrm{NH}) = 1.012$ Å, $A(\mathrm{HNH}) = 106.7°$. As the basis set size increases, the dipole moments converge to the same answer. For the grid-free approach, a triple zeta basis set is necessary to adequately represent the resolution of the identity, based on the agreement of grid and grid-free approaches. A quadruple zeta basis for water and a pentuple zeta basis for ammonia is necessary to converge the dipole moment and energy. So, for these species, the resolution of the identity is converged with respect to basis set before the dipole moment is. These dipole moments are within 0.04 D of the experimentally observed[62] dipole moments of 1.85 D for H_2O and 1.47 D for NH_3.

E. The ammonia bend potential

The bend potential of NH_3 was studied initially with the *B*-null exchange functional and the $6-311++G(3d,3p)$ basis set.[64] The N–H bond distance was constrained to the optimal $X\text{-}\alpha$ ($\alpha = 2/3$) value of 1.0496 Å to match the previous work by Werpetinski and Cook.[22] Because the NH bond is optimized for the $X\text{-}\alpha$ functional, the gradient will never go to zero. The energy, net dipole moment, and root-mean-square (rms) cartesian gradient at each point along the bend angle from 55° to 90° in 0.5° increments are presented in Figs. 1–3, respectively. The dipole moments (Fig. 1) differ by no more than 0.116 D and 5.95%. The grid-free and grid based energies (Fig. 2) differ by 0.0606 hartree, but the shapes of the surfaces are very similar (the standard deviation of the energy difference between the curves is 0.000 73 hartree). This suggests that for this size basis set the grid-free approach gives reliable relative energies, even though the absolute energies are too high. The rms gradient is significantly different (Fig. 3); this is probably a result of errors introduced by the resolution of the identity, particularly applying it to derivatives in Eqs. (13) and (18). Uncontracting the $6-311++G(3d,3p)$ basis set improves the fitting of the resolution of the identity, and therefore the quality of the grid-free results. To further explore these issues, the systematic correlation consistent basis sets of Dunning are

TABLE VIII. CH_2 geometry optimizations with B-VWN5 functional.

	Singlet energy (hartree)	Singlet bond distance (Å)	Singlet HCH angle	Triplet energy (hartree)	Triplet bond distance (Å)	Triplet HCH angle	Triplet-singlet splitting (eV)
aug-cc-pVTZ basis							
Hartree–Fock	−38.892 71	1.096	103.6°	−38.932 68	1.070	129.5°	−1.09
Grid	−39.378 03	1.115	101.0°	−39.391 97	1.079	134.0°	−0.38
Grid free	−39.450 45	1.411	60.5°	−39.455 21	1.253	82.3°	−0.13
Uncontracted *S*							
Grid	−39.378 88	1.115	101.0°	−39.392 71	1.079	133.9°	−0.38
Grid free	−39.237 49	1.134	93.8°	−39.266 04	1.079	136.6°	−0.78
Uncontracted							
Grid	−39.378 95	1.115	101.0°	−39.392 76	1.079	133.9°	−0.38
Grid free	−39.344 17	1.121	98.8°	−39.358 17	1.081	134.6°	−0.38
+2 more polarization							
Grid	−39.380 12	1.114	101.2°	−39.393 19	1.079	134.0°	−0.36
Grid free	−39.355 78	1.119	100.0°	−39.369 99	1.080	135.3°	−0.39
aug-cc-pVQZ basis							
Grid	−39.382 32	1.113	101.4°	−39.395 67	1.079	134.0°	−0.36
Grid free	−39.319 40	1.111	102.7°	−39.334 94	1.079	134.2°	−0.42
Uncontracted							
Grid	−39.382 43	1.113	101.4°	−39.395 77	1.079	134.1°	−0.36
Grid free	−39.364 37	1.122	98.7°	−39.377 46	1.081	132.5°	−0.36
+2 more polarization							
Grid free	−39.370 65	1.115	101.1°	−39.384 26	1.079	133.8°	−0.37

TABLE IX. C_3H_6 geometry optimizations with B-VWN5 functional.

	Propene energy (hartree)	Propene C=C bond distance (Å)	Propene C–C bond distance (Å)	Cyclopropane energy (hartree)	Cyclopropane C–C bond distance (Å)	Cyclopropane H–C bond distance (Å)	Energy difference (eV)
Hartree–Fock	−117.108 688	1.317	1.511	−117.096 518	1.498	1.073	−0.33
Grid	−118.604 631	1.338	1.524	−118.588 178	1.521	1.083	−0.45
Grid free	−118.457 918	1.328	1.544	−118.456 606	1.544	1.084	−0.04
Uncontracted							
Grid	−118.607 912	1.339	1.524	−118.591 789	1.520	1.083	−0.44
Grid free	−118.540 559	1.339	1.526	−118.523 173	1.525	1.088	−0.47

utilized.[63] The energy for basis sets that fail to adequately resolve the identity can be too low (Fig. 4). Therefore, just as an inadequate grid can give nonvariational and erratic energies and properties, an inadequate basis set to represent the resolution of the identity can suffer from the same problem. Grid-free results for all but the *cc-p*QZV basis set give incorrectly shaped rms gradient curves (Fig. 5). To further explore the resolution of the identity, the *cc-p*TZV basis set is systematically uncontracted (Figs. 6 and 7), because *cc-p*TZV gave the worst rms gradient curves. By uncontracting the valence *p* shell on the nitrogen the resolution of the identities in Eqs. (13) and (18) are more correctly represented. By further uncontracting the *s* shell on the hydrogen the resolution of the identity is better fit and the curves become more reasonable, although the minimum rms gradient is mispositioned by 5°.

F. Electronic states of triatomics

The $^1A_1$ and $^3B_1$ states of CH_2[65] are compared in Table VIII for both B-VWN5 and Hartree–Fock using an *aug-cc-p*VTZ[63] basis set. The $^3B_1$ state is optimized with a restricted open shell wave function. Table VIII shows that a basis set that is well designed for modeling occupied molecular orbitals, is not necessarily well designed to converge the resolution of the identity. For CH_2, the *aug-cc-p*VTZ basis set is too contracted to adequately represent the resolution of the identity. Uncontracting the *s* functions and then the *p* functions results in more sensible predicted properties. Additional sets of polarization functions (one set of more diffuse *d*'s and one set of tighter *d*'s on C and one set of more diffuse *p*'s and one set of tighter *p*'s on H), improve the resolution of the identity in Eqs. (13) and (18). Results for the quadruple zeta basis set show a similar trend, with the additional polarization functions agreeing with the grid based approach. Unlike Hartree–Fock, the B-VWN5 results agree with the experimentally observed splitting of 0.369–0.390 eV (8.5–9.0 kcal/mol),[66,66] and the experimental geometries[67] of 1.11 Å, 102° for $^1A_1$ and 1.07 Å, 134° for $^3B_1$.

G. Isomers of polyatomics

The geometries and energies of cyclopropane and propene[68] are compared in Table IX using both Hartree–Fock and B-VWN5 with a $6-311++G(3d,3p)$ basis set.[64] Although the grid-free approach gives reasonable geometries, it badly underestimates the energy difference. By uncontracting the basis set, and thus increasing the accuracy of the resolution of the identity, the grid-free approach, gives reasonable geometries and energy differences. The experimental $\Delta H_{298.15}$ is about 1.7 eV, with zero point energy (ZPE) corrections predicted to be significant.[68] While direct comparison with experimental values is not entirely appropriate, both the grid based and the grid-free results appear to be poor.

IV. CONCLUSIONS

The grid-free approach to DFT provides an alternative to the grid based approach to DFT. The resolution of the identity[69] (especially for gradient corrected functionals and energy gradient calculations) requires a more accurate basis set than does the wave function. The use of such large basis sets results in the calculation of a large number of two-electron integrals that are not otherwise needed. A more efficient approach will be to augment the atomic basis set with auxiliary functions only during the DFT part of the calculation. The vast knowledge base available for dealing with *wave function* basis set completeness in DFT[70] appears to be inadequate for addressing this issue, particularly for gradient corrected functionals. Previous work on auxiliary basis sets has dealt with the fitting of the $n^{1/3}X$-α potential[71] or the Coulomb potential.[72] Little or no work has been done on fitting the gradient of the density as in Eq. (13) or fitting the resolution of the identity between the alpha density and the beta density as in Eq. (15).

ACKNOWLEDGMENTS

This work was supported in part by grants from the Air Force Office of Scientific Research (F49-620-95-1-0073) and by the Ames Laboratory, U.S.-DOE. The authors would like to thank Dr. Mike Schmidt for many enlightening conversations. We would also like to thank the late Professor Jan Almlöf and Y. C. Zheng for providing us with an early version of the grid-free code in SUPERMOLECULE for comparisons to the GAMESS grid-free code.

APPENDIX A: PROOF OF EQUATION 7

$\tilde{M}[f(n)]$ is in an orthonormal basis in which $\tilde{M}[n]$ is diagonal (i.e., $\tilde{M}[n]=\lambda$)

$$\tilde{M}[f(n)]=\tilde{M}\left[\sum_m \alpha_m n^m\right],$$

series expansion of the function

$$=\sum_m \alpha_m \tilde{M}[n^m]$$

$$=\sum_m \alpha_m (\tilde{M}[n])^m,$$

by the resolution of the identity (exact in complete basis)

$$=\sum_m \alpha_m \lambda^m, \text{ since } \tilde{M}[n] \text{ is diagonal}$$

$$\tilde{M}[f(n)]=f(\lambda).$$

This should not be confused with the commonly used relationship, which is true in any basis:

$$f(\tilde{M}[n])=f(\lambda).$$

APPENDIX B: APPROXIMATE THREE-CENTER APPROACH

Expand the density in an orthonormal basis set

$$M[n]\approx M\left[\sum_{m=1}^{K} C_m \theta_m\right],$$

$$M[n]_{i,j}=\int \chi_i \sum_{m=1}^{K} C_m \theta_m \chi_j d\mathbf{r}.$$

Because $\{\theta\}$ is orthonormal, the expansion coefficients are given by

$$C_m=\int n\cdot\theta_m d\mathbf{r},$$

$$C_m=\sum_{r,s}^{\mathrm{AO}} D_{r,s}\int \chi_r\chi_s\theta_m d\mathbf{r}.$$

Substituted into $M[n]_{i,j}$ gives

$$M[n]_{i,j}=\int \chi_i \sum_{m=1}^{K}\left(\sum_{r,s}^{\mathrm{AO}} D_{r,s}\int \chi_r\chi_s\theta_m d\mathbf{r}\right)\theta_m\chi_j d\mathbf{r},$$

which rearranges to give

$$M[n]_{i,j}=\sum_{r,s}^{\mathrm{AO}}\sum_{m=1}^{K} D_{r,s}\int \chi_i\chi_j\theta_m d\mathbf{r}\cdot\int \theta_m\chi_r\chi_s d\mathbf{r},$$

which is equivalent to just applying the resolution of the identity.

APPENDIX C: $X-\alpha$ FUNCTIONAL ENERGY

For the closed shell $X-\alpha$ functional f, with molecular orbitals ψ

$$\hat{K}^{\mathrm{DFT}}_{v,\nu}=\int \psi_v\psi_\nu \frac{\partial f}{\partial n} d\mathbf{r},$$

$$\hat{K}^{\mathrm{DFT}}_{v,\nu}=C_{\alpha\frac{4}{3}}\int \psi_v\psi_\nu n^{1/3} d\mathbf{r}.$$

Forming the dot product of the DFT Fock matrix with the diagonal density matrix yields

$$\hat{K}^{\mathrm{DFT}}\cdot D=\sum_{v}^{\text{occupied}} 2\cdot C_{\alpha\frac{4}{3}}\int \psi_v\psi_v n^{1/3} d\mathbf{r},$$

$$\hat{K}^{\mathrm{DFT}}\cdot D=C_{\alpha\frac{4}{3}}\int n^{4/3} d\mathbf{r},$$

$$\hat{K}^{\mathrm{DFT}}\cdot D=\tfrac{4}{3}\cdot E^{\mathrm{DFT}}.$$

This is not the DFT energy.

[1] J. C. Slater, Adv. Quantum Chem. **6**, 1 (1972).
[2] S. H. Vosko, L. Wilk, and M. Nusair, Can. J. Phys. **58**, 1200 (1980).
[3] D. C. Langreth and M. J. Mehl, Phys. Rev. B **28**, 1909 (1983).
[4] M. Rasolt and D. J. W. Geldhart, Phys. Rev. B **34**, 1325 (1986).
[5] P. Hohenberg and W. Kohn, Phys. Rev. **136**, B864 (1964).
[6] J. P. Perdew, K. Burke, and M. Ernzerhof, J. Chem. Phys. **105**, 9982 (1996).
[7] A. D. Becke, J. Chem. Phys. **104**, 1040 (1996).
[8] B. I. Dunlap, Chem. Phys. **125**, 89 (1988).
[9] B. I. Dunlap, Phys. Rev. A **19**, 2902 (1984).
[10] B. G. Johnson, P. M. W. Gill and J. A. Pople, J. Chem. Phys. **98**, 5612 (1993).
[11] G. E. Scuseria, J. Chem. Phys. **97**, 7528 (1992).
[12] T. G. Wright, J. Chem. Phys. **105**, 7579 (1996).
[13] S. Gronert, G. N. Merrill, and S. R. Kass, J. Org. Chem. **60**, 488 (1995).
[14] H. M. Sulzbach, H. F. Schaefer, III, W. Klopper, and H. P. Lüthi, J. Am. Chem. Soc. **118**, 3519 (1996).
[15] R. G. Parr and W. Wang, *Density-Functional Theory of Atoms and Molecules* (Oxford, New York, 1989), Sec. III.
[16] A. I. M. Rae, Chem. Phys. Lett. **18**, 574 (1972).
[17] B. G. Johnson, C. A. Gonzales, P. M. W. Gill, and J. A. Pople, Chem. Phys. Lett. **221**, 100 (1994).
[18] V. I. Lebedev, Zh. Vychisl. Mat. Mat. Fiz. **15**, 48 (1975).
[19] V. I. Lebedev, Zh. Vychisl. Mat. Mat. Fiz. **16**, 293 (1975).
[20] P. M. W. Gill, B. G. Johnson, J. A. Pople, and M. J. Frisch, Chem. Phys. Lett. **197**, 499 (1992).
[21] B. I. Dunlap, J. Phys. Chem. **90**, 5524 (1986).
[22] K. S. Werpetinski and M. Cook, Phys. Rev. A **52**, R3397 (1995).
[23] Y. C. Zheng and J. Almlöf, Chem. Phys. Lett. **214**, 397 (1993).
[24] Y. C. Zheng and J. Almlöf, J. Mol. Struct.: THEOCHEM **288**, 277 (1996).
[25] K. S. Werpetinski and M. Cook, J. Chem. Phys. **106**, 7124 (1997).
[26] M. W. Schmidt, K. K. Baldridge, J. A. Boatz, S. T. Elbert, M. S. Gordon, J. H. Jensen, S. Koseki, N. Matsunaga, K. A. Nguyen, S. Su, T. L. Windus, M. Dupuis, and J. A. Mongomery, Jr., J. Comput. Chem. **14**, 1347 (1993).
[27] O. Vahtras, J. Almlöf, and M. W. Feyereisen, Chem. Phys. Lett. **213**, 514 (1993).
[28] A. E. DePristo and J. D. Kress, J. Chem. Phys. **86**, 1425 (1987).
[29] B. A. Hess, R. J. Buenker, and P. Chandra, Int. J. Man-Mach. Stud. **29**, 737 (1986).
[30] S. Obara and A. Saika, J. Chem. Phys. **84**, 3963 (1986).
[31] A. M. Köster, J. Chem. Phys. **104**, 4114 (1996).
[32] W. von Niessen, Theor. Chim. Acta **27**, 9 (1972).
[33] W. von Niessen, J. Chem. Phys. **56**, 4290 (1971).
[34] J. Almlöf, in *Modern Electron Structure Theory Part 1*, edited by D. R. Yarkony (World Scientific, River Edge, NJ, 1995), p. 110.
[35] F. Herman, I. B. Ortenburger, and J. P. van Dyke, Int. J. Quantum Chem. **IIIS**, 827 (1970).
[36] R. Neumann and N. C. Handy, Chem. Phys. Lett. **266**, 16 (1997).
[37] K. Kobayashi, N. Kurita, H. Kumahora, and K. Tago, Phys. Rev. A **43**, 5810 (1991).
[38] R. Fournier, J. Chem. Phys. **92**, 5422 (1990).

[39] J. P. Perdew and Y. Wang, Phys. Rev. B **45**, 13244 (1992).
[40] B. G. Johnson, P. M. W. Gill, and J. A. Pople, Chem. Phys. Lett. **220**, 377 (1994).
[41] J. Baker, J. Andzelm, A. Scheiner, and B. Delley, J. Chem. Phys. **101**, 8894 (1994).
[42] V. Termath, D. J. Tozer, and N. C. Handy, Chem. Phys. Lett. **228**, 239 (1994).
[43] Equations (4) and (5) of Q. Zhao and R. G. Parr, Phys. Rev. A **46**, R5320 (1992).
[44] D. M. Ceperley and B. J. Alder, Phys. Rev. Lett. **45**, 466 (1980).
[45] Equation (24) of G. J. Laming, V. Termath, and N. Handy, J. Chem. Phys. **99**, 8765 (1993).
[46] E. P. Wigner, Phys. Rev. **46**, 1002 (1934).
[47] E. P. Wigner, Trans. Faraday Soc. **34**, 678 (1938).
[48] A. D. Becke, Phys. Rev. A **38**, 3098 (1988).
[49] B. Miehlich, A. Savin, H. Stoll, and H. Preuss, Chem. Phys. Lett. **157**, 200 (1989).
[50] C. Lee, W. Yang, and R. G. Parr, Phys. Rev. B **37**, 785 (1988).
[51] R. Colle and D. Salvetti, Theor. Chim. Acta **37**, 329 (1975).
[52] Gaussian 92/DFT, Revision G.3, M. J. Frisch, G. W. Trucks, H. B. Schlegel, P. M. W. Gill, B. G. Johnson, M. W. Wong, J. B. Foresman, M. A. Robb, M. Head-Gordon, E. S. Replogle, R. Gomperts, J. L. Andres, K. Raghavachari, J. S. Binkley, C. Gonzalez, R. L. Martin, D. J. Fox, D. J. Defrees, J. Baker, J. J. P. Stewart, and J. A. Pople, Gaussian, Inc., Pittsburgh PA, 1993.
[53] Int=FineGrid and SCF=tight. It is worth noting that this is the default grid in Gaussian 94.
[54] M. W. Schmidt and K. Ruedenberg, J. Chem. Phys. **71**, 3951 (1979).
[55] Exponents for higher angular momentum (d,f) were generated using the outermost shell exponents.
[56] K. P. Huber and G. Herzberg, *Constants of Diatomic Molecules* (Van Nostrand Reinhold, New York, 1979), p. 412.
[57] D. Sundholm, P. Pyykko, and L. Laaksonen, Mol. Phys. **56**, 1411 (1985).
[58] L. A. Curtiss, K. Raghavachari, G. W. Trucks, and J. A. Pople, J. Chem. Phys. **94**, 7221 (1991).
[59] X. W. Fan, X. J. Chen, S. J. Zhou, Y. Zheng, C. E. Brion, R. Frey, and E. R. Davidson, Chem. Phys. Lett. **276**, 346 (1997).
[60] M. P. C. M. Krijn and D. Feil, Chem. Phys. Lett. **150**, 45 (1988).
[61] J. S. Muenter, J. Mol. Spectrosc. **55**, 490 (1975).
[62] *Handbook of Chemistry and Physics*, edited by D. R. Lide, 74th ed. (CRC, Boca Raton, FL, 1993), pp. 9–42.
[63] T. H. Dunning, Jr., J. Chem. Phys. **90**, 1007 (1989).
[64] R. Krishnan, J. S. Binkley, R. Seeger, and J. A. Pople, J. Chem. Phys. **72**, 650 (1980).
[65] N. Matsunaga, S. Koseki, and M. S. Gordon, J. Chem. Phys. **104**, 7988 (1996).
[66] D. G. Leopold, K. K. Murray, A. E. Stevens Miller, and W. C. Lineberger, J. Chem. Phys. **83**, 4849 (1985).
[67] A. R. W. McKellar, P. R. Bunker, T. J. Sears, K. M. Evenson, R. J. Saykally, and S. R. Langhoff, J. Chem. Phys. **79**, 5251 (1983).
[68] K.-N. Fan, Z.-H. Li, W.-H. Li, W.-N. Wang, H.-H Huang, and W. Huang, Chem. Phys. Lett. **277**, 257 (1997).
[69] In this work, Eqs. (3b), (7), (13c), and (20).
[70] J. M. Martell, J. D. Goddard, and L. A. Eriksson, J. Phys. Chem. A **101**, 1927 (1997).
[71] N. Godbout, D. R. Salahub, J. Andzelm, and E. Wimmer, Can. J. Chem. **70**, 560 (1992).
[72] K. Eichkorn, O. Treutler, H. Öhm, M. Häser, and R. Ahlrichs, Chem. Phys. Lett. **240**, 283 (1995).